Control of DFIG based Wind Generation to Improve Inter-Area Oscillation Damping

Zhixin Miao, Lingling Fan, Dale Osborn, Subbaraya Yuvarajan

***Abstract*—In this paper, control of inter-area oscillation in power systems with high wind power penetration is achieved via doubly fed induction generator (DFIG). The DFIG is modeled in Matlab®/Simulink. A two-area system is investigated with a wind farm connected in the area that exports power. Control schemes for active power and reactive power regulation are designed firstly. The paper finds that without active power and reactive power regulation, it is impossible to design an effective inter-area oscillation damping controller through DFIG machine side inverter. An auxiliary control loop for oscillation damping that adjusts the active power command can help damp the inter-area oscillation. Time domain simulations demonstrate the effectiveness of the control.**

***Index Terms*—Wind Generation, Doubly Fed Induction Generator, Inter-Area Oscillation**

I. Introduction

THE demand for renewable energy increases day by day for the apparent concerns of energy shortage and global warming. In Europe and US, legislative acts have been enforced for renewable energy usage. Wind generation is one type of renewable energy resource that has been the focus of renewable energy profile in states with strong wind resources. California and Texas are the leading states to use wind energy and other states follow up. In Minnesota, 25% of renewable power penetration has been required by the state by 2025 [1].

Based on the electrical topology, wind turbine generators can be grouped into four categories [2]:

1) fixed-speed squirrel-cage induction generators
2) variable-slip (wound rotor) induction generators with variable rotor resistance
3) variable-speed doubly fed asynchronous generators
4) variable-speed generators with full converter interface

Compared with variable-speed wind generators, the fixed-speed type has both advantages and disadvantages. The key advantage of the variable-speed generator is its ability to extract maximum electric power at various wind speed via rotor speed adjusting. The variable speed generator reduces the mechanical stress imposed on the turbine. The fixed-speed generator has no ability to vary the rotor speed. Though it requires no complex power electronics interface, the fixed speed induction generator has low efficiency of wind power conversion and no ability to provide reactive power support. It also imposes tense mechanical stress on turbines and requires complex pitch control to maintain a constant rotor speed.

The doubly fed induction generator (DFIG) is the most popular type of variable speed generator and it is currently used in about 25% of wind turbine generation that are operating in the world. A detailed full-order DFIG model is necessary when the alternating rotor current considered in simulation [3]. In this paper, the full-order DFIG and the wind turbine with maximal power extracting capability will be modeled in Matlab®/Simulink. Furthermore, the DFIG-based wind generation will be modeled in a two-area four-machine test power system. The wind power penetration is assumed to be 20% in the area considered.

While long-distance power transfer requires sufficient reactive power, it could also cause inter-area oscillations. In real wind generation interconnection studies in upper midwest region, instability due to oscillation has already been observed. This paper will design the control of DFIG to provide damping of the inter-area oscillations. Due to the wind fluctuation, the power transfer levels and terminal voltages will vary. The robustness of the controller will be analyzed under wind fluctuation.

The paper is organized as follows. Section I is the introduction and the research objective of the paper. Section II describes the wind generation model. Section III presents the configuration of the test system. Section IV presents the difficulty of inter-area oscillation damping control without proper internal DFIG control and also introduces the control schemes for active power and reactive power regulation and inter-area oscillation damping. Section V presents the simulation results and discussion. Section VI concludes the paper.

II. The Wind Generation Model

The configuration of a grid-tied system with a DFIG and wind turbine is shown in Fig. 1. In the following subsections, the dynamic model and the steady state model of the wind turbine and the DFIG are expressed in mathematical form.

A. Wind Turbine Model

The dynamic output mechanical torque of the wind turbine is expressed [4], [5] as:

$$T_m = \frac{1}{2}\rho A R C_p V_\omega^2/\lambda \tag{1}$$

where, ρ is the air density, A is the blade sweep area, R is the rotor radius of wind turbine, and V_ω is wind speed. C_p is the power coefficient of the blade which is a function of the blade pitch angle θ, and the tip speed ratio as:

Z. Miao and D. Osborn are with transmission asset management department, Midwest ISO Inc, St. Paul MN 55108. email: Zhixin.Miao@ieee.org, DOsborn@midwestiso.org

L. Fan and S. Yuvarajan are with Dept. of Electrical & Computer Engineering, North Dakota State University, Fargo, ND 58105. Email: Lingling.Fan@ndsu.edu, SubSubbaraya.Yuvarajan@ndsu.edu

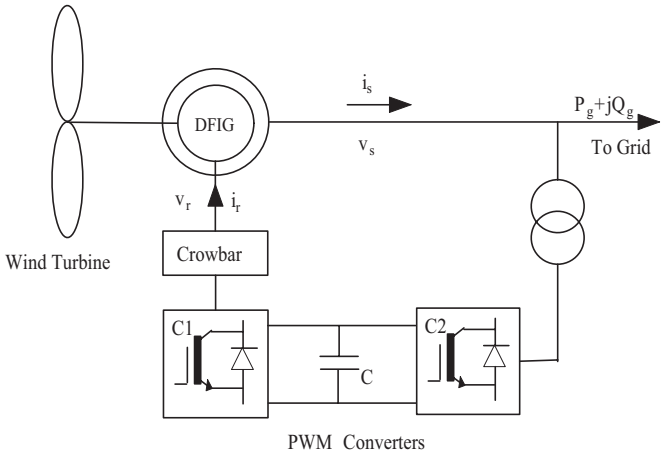

Fig. 1. Grid-tied DFIG wind turbine system.

$$C_p = (0.44 - 0.0167\theta)\sin\left(\frac{\pi(\lambda - 3)}{15 - 0.3\theta}\right) - 0.00184(\lambda - 3)\theta \tag{2}$$

and tip speed ratio λ is:

$$\lambda = \frac{\Omega R}{V_\omega} \tag{3}$$

where Ω is the mechanical angular velocity.

Fig. 2 illustrates the relationship of the power coefficient C_p, the tip speed ratio λ and the blade pitch angle θ in Eqn. 2. It is seen that to extract the maximum power from the wind turbine, the turbine speed has to be adjusted according to the wind speed. Therefore, it is energy efficient to use variable speed generators. The DFIG is one type of variable speed generator. For power system simulations involving grid disturbances, it

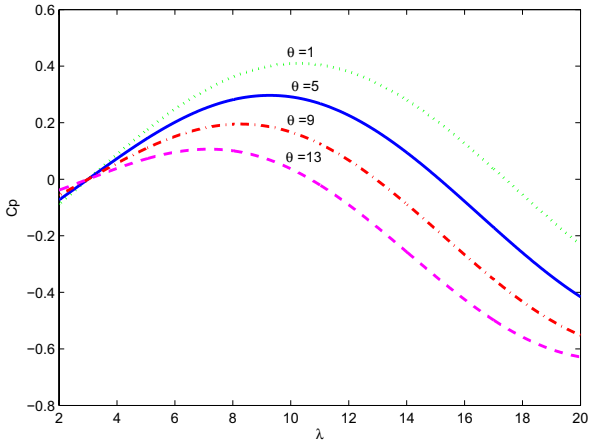

Fig. 2. Power coefficient versus speed.

is reasonable to assume that the wind speed remains constant for 5 to 30 seconds typical of such cases.

B. Wound Rotor Induction Generator

The DFIGs are wound rotor induction generators in which controllable rotor voltages can be injected. The injected rotor voltage has a variable frequency ω_{vr}. This AC voltage will generate a flux linkage with frequency ω_{vr} if the rotor is stand still. When the rotor is rotating a speed of ω_r, the final flux linkage generated by the rotor and the injected rotor voltage will have a frequency of $\omega_r + \omega_{vr}$ [6]. We want the final flux linkage to have a frequency of 60 Hz. From the relationship diagram of maximum power coefficient versus turbine speed and wind speed, we can find the desired rotor speed given a wind speed. Therefore, we can determine the frequency of the voltage to be injected as a function of the wind speed.

The voltage equations of an induction machine in the arbitrary reference frame can be written in terms of the currents as shown in Eqn. 4 [7]. The model of a wound rotor induction generator is different from that of a squirrel cage induction generator in which V_{qr} and V_{dr} are zero. In the case of a DFIG, the two variables V_{qr} and V_{dr} are controllable via the rotor side inverter.

In Eqn. 4, ω is the rotating speed of an arbitrary reference frame. If we select $\omega = \omega_b$, that is, the rotating speed of the reference frame is same as 60 Hz, then this reference frame is called a synchronously rotating reference frame.

Assume that the reference frame is synchronous reference frame and that all quantities are in per unit value. Eqn. 4 can be further written into $\dot{X} = AX + BU$, where $X = [i_{qs}, i_{ds}, i_{os}, i'_{qr}, i'_{dr}, i'_{0r}]^T$.

$$B = \begin{bmatrix} \frac{X_{ss}}{\omega_b} & 0 & 0 & \frac{X_M}{\omega_b} & 0 & 0 \\ 0 & \frac{X_{ss}}{\omega_b} & 0 & 0 & \frac{X_{ss}}{\omega_b} & 0 \\ 0 & 0 & \frac{X_{ss}}{\omega_b} & 0 & 0 & 0 \\ \frac{X_{ss}}{\omega_b} & 0 & 0 & \frac{X'_{rr}}{\omega_b} & 0 & 0 \\ 0 & \frac{X_{ss}}{\omega_b} & 0 & 0 & \frac{X'_{rr}}{\omega_b} & 0 \\ 0 & 0 & 0 & 0 & 0 & \frac{X'_{lr}}{\omega_b} \end{bmatrix}^{-1} \tag{5}$$

The swing equation is

$$T_e = 2H\dot{\omega}_r + T_m \tag{7}$$

The torque equation is

$$T_e = X_M(i_{qs}i'_{dr} - i_{ds}i'_{qr}) \tag{8}$$

C. Initialization of DFIG

To initialize the DFIG model for time domain simulation, we only need to know the initial wind speed or wind torque. The initialization is actually simpler than the initialization of a squirrel cage induction machine. In the case of a squirrel cage induction generator, the initial condition of the induction machine such as the rotor speed ω_r and absorbed reactive power Q should be computed from the known variables: active power P and terminal voltage phasor $\bar{V}$. The rotor speed can be calculated by Newton-Raphson method [8].

The steady state equivalent circuit of an induction machine is shown in Fig. 3.

Given the initial wind speed, we can obtain the optimal rotor speed ω_r from turbine speed versus maximum electric power relationship. We should also know the initial active power and reactive power scheduling P and Q as well as

$$\begin{bmatrix} v_{qs} \\ v_{ds} \\ v_{0s} \\ v'_{qr} \\ v'_{dr} \\ v'_{0r} \end{bmatrix} = \begin{bmatrix} r_s + \frac{p}{\omega_b}X_{ss} & \frac{\omega}{\omega_b}X_{ss} & 0 & \frac{p}{\omega_b}X_M & \frac{\omega}{\omega_b}X_M & 0 \\ -\frac{\omega}{\omega_b}X_{ss} & r_s + \frac{p}{\omega_b}X_{ss} & 0 & -\frac{\omega}{\omega_b}X_M & \frac{p}{\omega_b}X_M & 0 \\ 0 & 0 & r_s + \frac{p}{\omega_b}X_{ls} & 0 & 0 & 0 \\ -\frac{p}{\omega_b}X_M & \frac{\omega-\omega_r}{\omega_b}X_M & 0 & r'_r + \frac{p}{\omega_b}X'_{rr} & \frac{\omega-\omega_r}{\omega_b}X_M & 0 \\ -\frac{\omega-\omega_r}{\omega_b}X_M & \frac{p}{\omega_b}X_M & 0 & -\frac{\omega-\omega_r}{\omega_b}X'_{rr} & r'_r + \frac{p}{\omega_b}X'_{rr} & 0 \\ 0 & 0 & 0 & 0 & 0 & r'_r + \frac{p}{\omega_b}X'_{lr} \end{bmatrix} \begin{bmatrix} i_{ds} \\ i_{qs} \\ i_{0s} \\ i'_{qr} \\ i'_{dr} \\ i'_{0r} \end{bmatrix} \tag{4}$$

$$A = -B \begin{bmatrix} r_s & \frac{\omega}{\omega_b}X_{ss} & 0 & 0 & \frac{\omega}{\omega_b}X_M & 0 \\ -\frac{\omega}{\omega_b}X_{ss} & r_s & 0 & -\frac{\omega}{\omega_b}X_M & 0 & 0 \\ 0 & 0 & r_s & 0 & 0 & 0 \\ 0 & \frac{\omega-\omega_r}{\omega_b}X_M & 0 & r'_r & \frac{\omega-\omega_r}{\omega_b}X_M & 0 \\ -\frac{\omega-\omega_r}{\omega_b}X_M & 0 & 0 & \frac{\omega-\omega_r}{\omega_b}X'_{rr} & r'_r & 0 \\ 0 & 0 & 0 & 0 & 0 & r'_r \end{bmatrix} \tag{6}$$

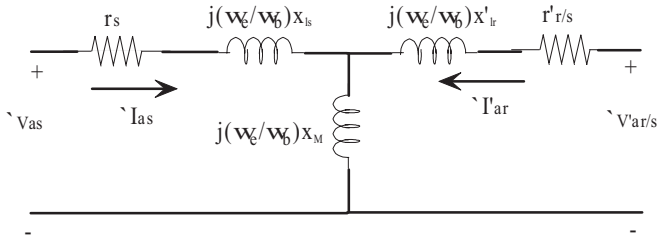

Fig. 3. Steady State Motor Circuit.

the initial terminal voltage V_s. Therefor, the rotor side voltage phasor should be

$$V_r/s = V_s - I_s(R_s + jX_{ls}) + I_r(R_r/s + jX_{lr})$$

where $s = (\omega_b - \omega_r)/\omega_b$, ω_b is the nominal speed at 60 Hz,

$$I_s = \frac{P - jQ}{V_s^*}$$

and

$$I_r = I_s + \frac{V_s - I_s(R_s + jX_{ls})}{jX_M}$$

Compared with squirrel cage induction generator initialization, here no iteration is needed and can directly compute V_{qr} and V_{dr}.

III. Configuration of Test System

The test system shown in Fig. 4 is based on the classic two-area four-machine system developed in [9] for inter-area oscillation analysis. In Area 1, a wind farm is connected to the grid. The wind farm penetration is assumed to be 20% of Area 1.

Area 1 has two synchronous generators, each with 835 MW rated power. Gen 1 exports 700 MW and Gen 2 exports 560 MW. The exporting power level of the wind farm is 240 MW - about 20% of 1260 MW. Area 2 also has two synchronous generators, each with 835 MW rated power. All four synchronous generators are identical. In this paper, the full-order model of synchronous generator is used. The parameters of the steam turbine generators come from Krause's classic textbook

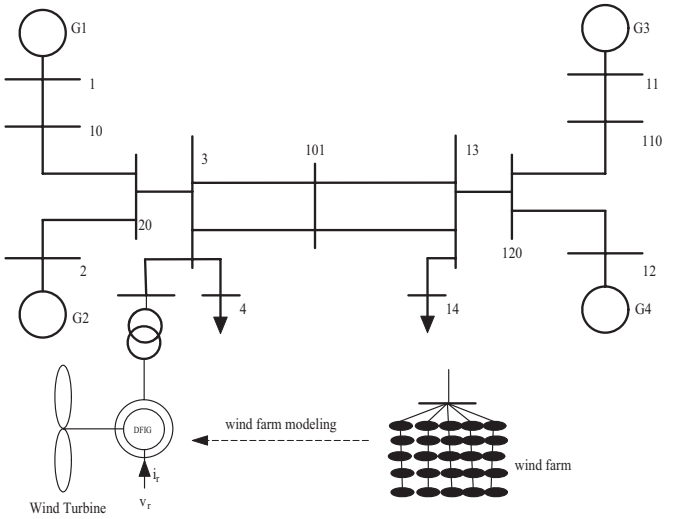

Fig. 4. One-line diagram of two-area system with wind generator.

Analysis of Electric Machinery [7]. The parameters are also shown in Table II in Appendix.

The inter-area oscillation is characterized as the swing of the generators in Area 1 against the generators in Area 2 and the frequency of the oscillation is about 0.72 Hz or 4.53 rad/s.

IV. Control of DFIG

Without any internal mode control, such as PQ tracking, the DFIG model is actually not stable [10], [11]. This can also be confirmed from the root locus diagram in Fig. 5. The input of the open loop system is the q-axis rotor voltage V_{qr}. The output of the open loop system is the rotor angle difference between the synchronous generator 2 and 3. This output signal should have a good observability of the inter-area oscillation mode between the two areas [12]. The angle difference signal can be obtained through state-of-art Phasor Measurement Unit technology. In this paper, we assume that the angle difference signal is available. From the root locus diagram, we can observe that there are poles and zeros at right half plane (RHP). It is very difficult to design controller using the input/output pair due to the RHP poles and zeros.

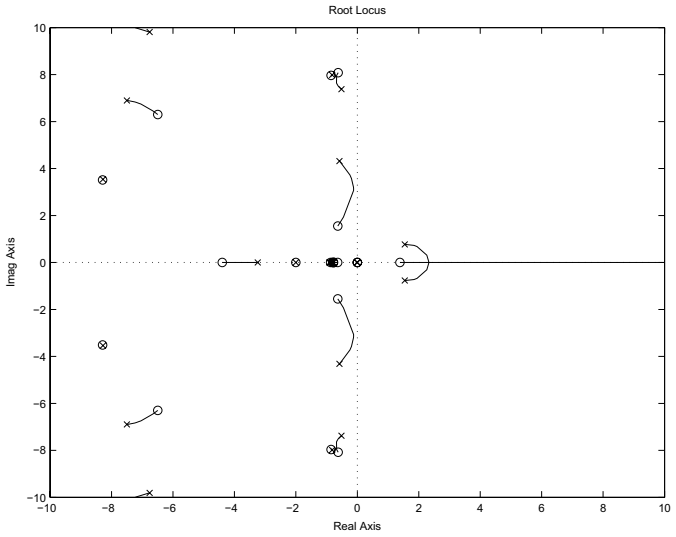

Fig. 5. Root locus diagram of the open loop system.

Instead, the first step of damping controller design should make the internal DFIG model stable. This can be achieved by PQ tracking. Active power and reactive power tracking can be achieved by PI controller. Federal Energy Regulatory Commission (FERC) Orders 661 requires wind plants to have the capability to control their reactive power within 0.95 leading to 0.95 lagging range [2]. Therefore the capability of PQ tracking is necessary.

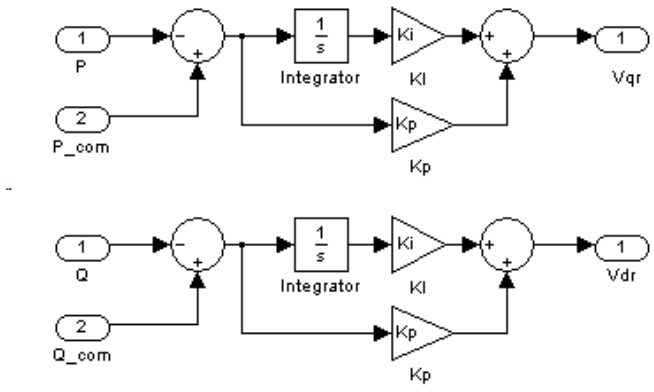

Fig. 6. Control of PQ tracking.

The PQ tracking controllers are PI controllers shown in Fig. 6. We adjust V_{qr} based on P and adjust V_{dr} based on Q. After PQ tracking, the root locus diagram is shown in Fig. 8. There is no RHP poles and zeros. It is now possible to design a controller based on the root locus diagram. In this case, we can place a zero on the left real axis to attract the root locus from the the dominant mode with 4.3 rad/s frequency. We should also place a pole on the left real axis to make the controller proper, which means the number of poles is greater than or equal the number of the zeros. The controller has the following transfer function:

$$K(s) = \frac{1+2s}{1+0.32s}$$

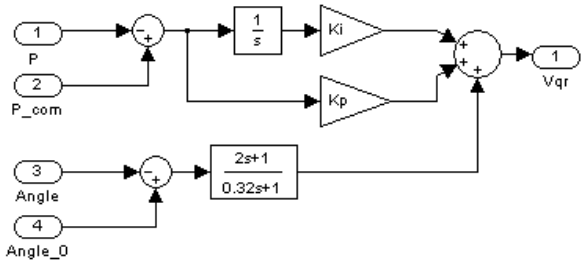

Fig. 7. Damping control scheme.

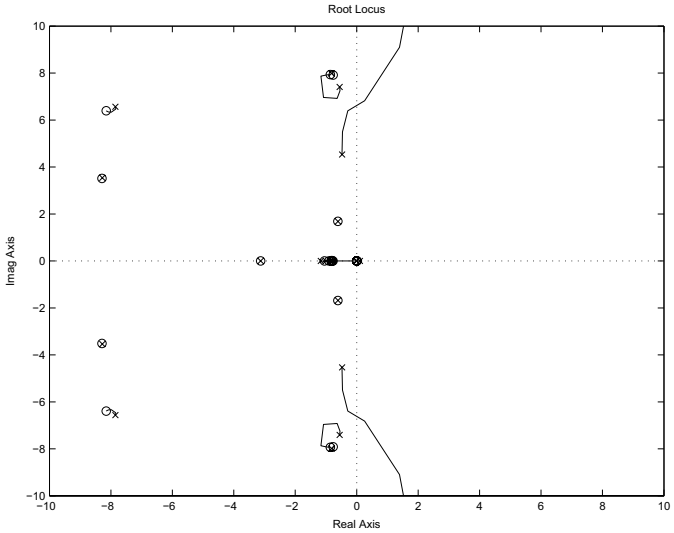

Fig. 8. Root locus diagram of the system with PQ tracking.

With this controller, the damping of the inter-area oscillation is improved.

V. Simulations and Discussion

Simulations are performed on the test system. The system will operate under steady state for 1 second. The power transfer between the two areas is 400 MW. A temporary three-phase fault occurs at Bus 3 and is cleared after 0.3 second. Fig. 9 and Fig. 10 show the dynamic responses of the synchronous generators and the DFIG. In Fig. 9, the relative angle differences, rotor speeds and electric power exporting levels are plotted. In Fig. 10, the DFIG rotor speed, DFIG mechanical torque, electric torque and terminal voltage are plotted. It is to be noted that the mechanical torque is adjusted by pitch control.

Fig. 11 and Fig. 12 are simulation plots when PQ tracking controllers are available. These controllers are PI controllers. It is found that with PQ tracking control, the DFIG rotor speed

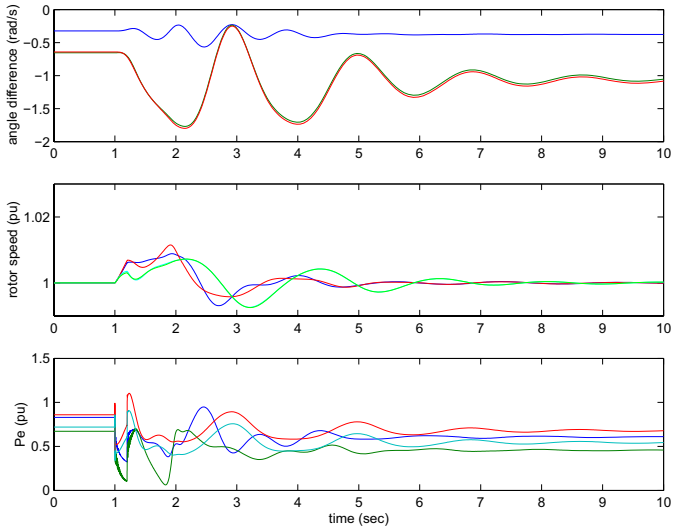

Fig. 9. Dynamic responses of the synchronous generators with no control

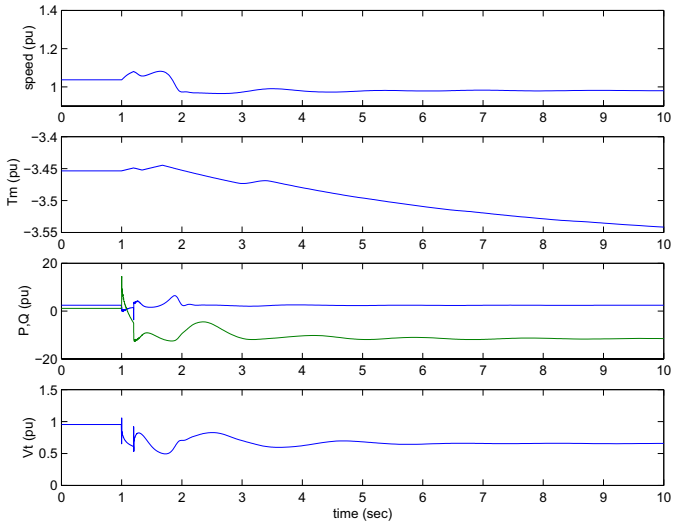

Fig. 10. Dynamic responses of the DFIG with no control.

is kept to the original operating condition after the fault. Also the oscillation observed in the synchronous generator relative angle has been suppressed.

Fig. 13 and Fig. 14 show the dynamic responses of the synchronous generators and the induction generator with the auxiliary damping control added to DFIG rotor voltage.

Due to the difference in scale, it is difficult to observe the difference between the relative angle dynamic responses. Hence the dynamic responses of the rotor angle of Gen 3 relative to Gen 1 are plotted together for the three scenarios: 1) constant V_{qr}, V_{dr} or no control; 2) PQ tracking; 3) PQ tracking and damping control. The plots are shown in Fig. 15. From the plots, we can tell without PQ tracking control, the original operating condition cannot be recovered. Besides the swing magnitude of the system without DFIG control is much greater than the swing magnitude of the system with PQ tracking. It is also found that the auxiliary damping control loop can enhance the inter-area oscillation damping.

The corresponding eigenvalues of the inter-area oscillation

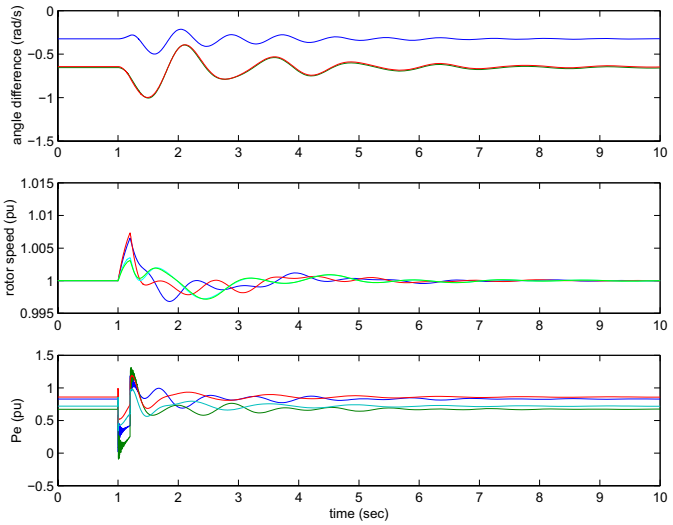

Fig. 11. Synchronous generator dynamic responses with PQ tracking.

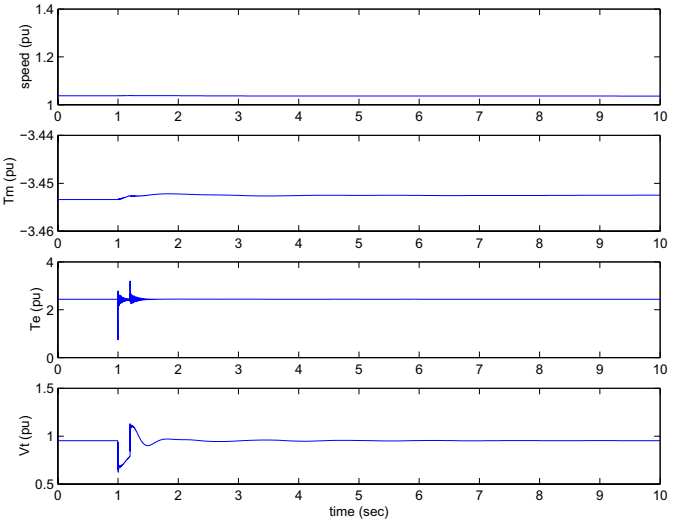

Fig. 12. Wind turbine generation dynamic responses with PQ tracking.

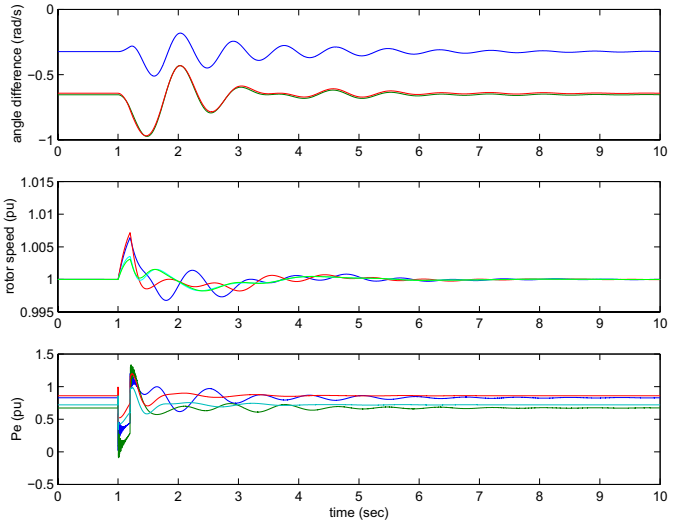

Fig. 13. Synchronous generator dynamic responses with PQ tracking and damping control.

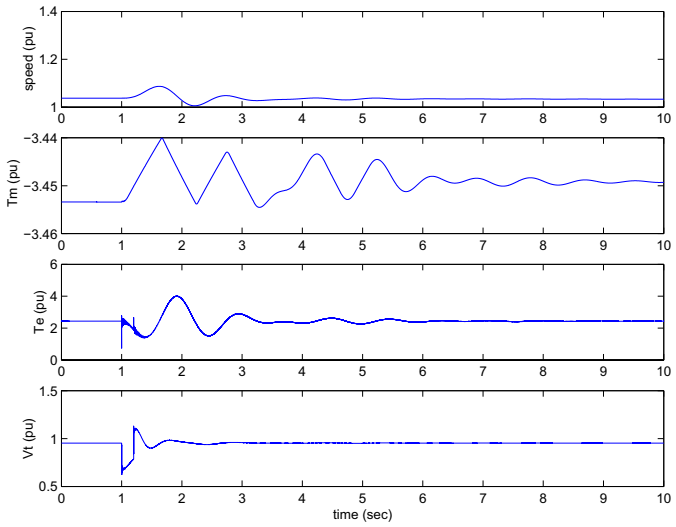

Fig. 14. Wind turbine generator dynamic responses with PQ tracking and damping control.

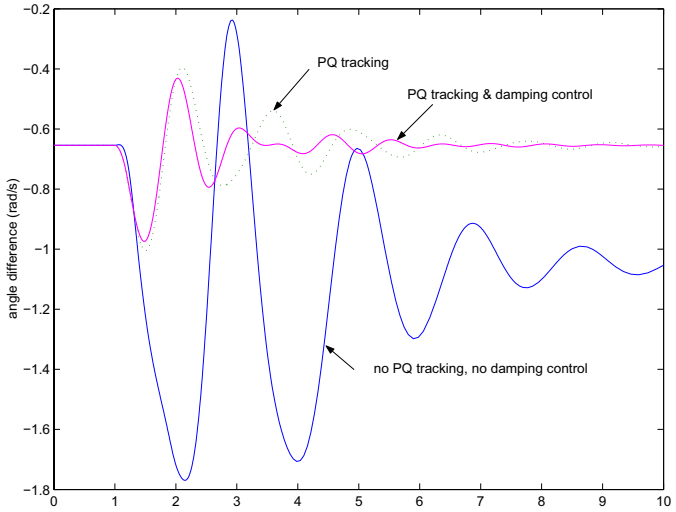

Fig. 15. Angle difference dynamic responses comparison.

at two scenarios (Case 1: with PQ tracking only; Case 2: with PQ tracking and damping control) are listed in Table I.

VI. Conclusion

In this paper, the control of the machine side converter of DFIG based wind turbine generation is designed to improve inter-area oscillation damping in a high-penetration power system scenario. The DFIG and the wind turbine are modeled in Matlab®/Simulink. A two-area system is investigated with a wind farm connected in the area that exports power. Control schemes for active power and reactive power regulation and inter-area oscillation damping are designed. Time domain simulations demonstrate the effectiveness of the control.

TABLE I
Inter-Area Oscillation Mode in Two Scenarios

Case	Eigenvalue	Frequency(Hz)	Damping
Case 1	$-0.4745 \pm j4.5312$	0.7212	10.41%
Case 2	$-0.8069 \pm j5.1737$	0.8234	15.41%

TABLE II
Synchronous Generator Parameters

Rating: 835 MVA
Line to line voltage: 26 kV
Power factor: 0.85
Poles: 2
Speed: 3600 r/min
Combined inertia of generator and turbine: H = 5.6 s
$r_s = 0.00243\Omega, 0.003$ pu
$X_{ls} = 0.1538\Omega, 0.19$ pu

$X_q = 1.457\Omega, 1.8$pu	$X_d = 1.457\Omega, 1.8$pu
$r'_{kq1} = 0.00144\Omega, 0.00178$pu	$r'_{fd} = 0.00075\Omega, 0.000929$pu
$X'_{lkq1} = 0.6578\Omega, 0.8125$pu	$X'_{lfd} = 0.1165\Omega, 0.1414$pu
$r'_{kq2} = 0.00681\Omega, 0.00841$pu	$r'_{kd} = 0.01080\Omega, 0.01334$pu
$X'_{lkq2} = 0.07602\Omega, 0.0939$pu	$X'_{lkd} = 0.06577\Omega, 0.08125$pu

Appendix

The synchronous generator parameters of the test system are listed in Table II.

The induction generator parameters are: $H = 5$s, $r_s = 0.00059$pu, $X_M = 0.4161$pu, $r_r = 0.00339$pu, $X_{ls} = 0.0135$pu, $X_{lr} = 0.0075$pu.

Acknowledgment

The authors would like to thank Dr. Jacob Glower, Professor of Electrical & Computer Engineering, North Dakota State University for his help on controller design using root locus approach.

References

[1] "Final report - 2006 Minnesota wind integration study," The Minnesota Public Utilities Commission, St. Paul, Minnesota, Tech. Rep., May 2007.
[2] R. Zavadil, N. Miller, A. Ellis, and E. Muljadi, "Queuing up," *IEEE Power Energy Mag.*, vol. 5, pp. 47–58, November/December 2007.
[3] I. Erlich, J. Kretschmann, J. Fortmann, S. Mueller-Engelhardt, and H. Wrede, "Modeling of wind turbines based on doubly-fed induction generators for power system stability studies," *IEEE Trans. Power Syst.*, vol. 22, pp. 909–919, Aug. 2007.
[4] E. Abdin and W. Xu, "Control design and dynamic performance analysis of a wind turbine induction generator unit," *IEEE Trans. Energy Convers.*, vol. 15, Mar. 2000.
[5] A. Murdoch, R. Barton, and J. W. S. Javid, "Control design and performance analysis of a 6 mw wind turbine-generator," *IEEE Trans. Power App. Syst.*, vol. 102, pp. 1340–1347, May 1983.
[6] S. Muller, M. Deicke, and R. W. D. Doncker, "Doubly fed induction generator systems for wind turbine," *IEEE Ind. Appl. Mag.*, pp. 26–33, May/June 2002.
[7] P. Krause, *Analysis of Electric Machinery*. New York: McGraw-Hill, 1986.
[8] Z. Miao, "Modeling and dynamic stability of distributed generations," Ph.D. dissertation, West Virginia University, 2002.
[9] M. Klein, G. Rogers, and P. Kundur, "A fundamental study of inter-area oscillations in power systems," *IEEE Trans. Power Syst.*, vol. 6, pp. 914–921, Aug. 1991.
[10] T. K. A. Brekken and N. Mohan, "Control of a doubly fed induction wind generator under unbalanced grid voltage conditions," *IEEE Trans. Energy Convers.*, vol. 22, pp. 129–135, March 2007.
[11] A. Petersson, "Analysis, modeling and control of doubly fed induction generators for wind turbines," Ph.D. dissertation, Chalmers Unv. of Technol., Gothenburg, Sweden, 2005.
[12] E. Larsen, J. J. Sanchez-Gasca, and J. Chow, "Concepts for design of facts controllers to damp power swings," *IEEE Trans. Power Syst.*, vol. 10, pp. 948–956, May 1995.

Zhixin Miao received his BSEE from Huazhong University of Science & Technology, Wuhan, China, in 1992. He received his MSEE from the graduate school of Nanjing Automation Research Institute in 1997 and Ph.D. in Electrical Engineering from West Virginia University. He is with transmission asset management department in Midwest ISO, St. Paul, Minnesota since 2002. His research interests include dynamics modeling of electric machinery and power system, power system protection, reliability and economics.

Lingling Fan is an assistant professor in Dept. of Electrical & Computer Engineering, North Dakota State University. She received the BS, MS degrees in electrical engineering from Southeast University, Nanjing, China, in 1994 and 1997, respectively. She received Ph.D. degree in electrical engineering from West Virginia University in 2001. Before joining NDSU, Dr. Fan was with Midwest ISO, St. Paul, Minnesota. Her research interests include control of renewable energy resources, protection of power systems, power system reliability and economics.

Dale Osborn was born in Nebraska in 1945. He received his Bachelor and Master from University of Nebraska. He was the manager of planning department of NPPD. He was reactive power management manager in ABB from 1990-2000. Currently he is the technical director of transmission asset management department in Midwest ISO. His research interests cover power system planning, reliability, economics and reactive power device manufacturing.

Subbaraya Yuvarajan received his Ph.D. degree in Electrical Engineering from Indian Institute of Technology, Chennai, India in 1981. He received his M. Tech degree from Indian Institute of Technology in 1969 and B.E (Hons) degree from University of Madras in 1966. Dr. Yuvarajan has been a Professor of Electrical and Computer Engineering at NDSU from 1995. His research areas are Electronics, Power Electronics and Electrical Machines.